J Polym Res (2010) 17:579–588
DOI 10.1007/s10965-009-9346-z

ORIGINAL PAPER

Preparation of gold nanoparticles under presence of the diblock polyampholyte PMAA-*b*-PDMAEMA

Boris Mahltig · Nicolas Cheval · Jean-Francois Gohy · Amir Fahmi

Received: 4 June 2009 / Accepted: 17 September 2009 / Published online: 28 October 2009

Abstract The preparation of gold nanoparticles in presence of different weak polyampholytes is investigated. As diblock polyampholytes several poly(methacrylic acid)-*block*-poly((dimethylamino)ethyl methacrylate), PMAA-*b*-PDMAEMA, have been used, characterized by different molecular weight and block ratio. $HAuCl_4$ is used as gold precursor where $LiBH_4$ is acting as reductive agent to obtain the gold nanoparticles. The addition of gold precursors to aqueous solutions of PMAA-*b*-PDMAEMA polyampholytes leads to an acidification of the solution resulting in a change of the polyampholyte conformation through protonation of the PDMAEMA blocks. This modification of polyampholyte conformation also allows the tuning of the size and size distribution of the accordingly formed gold nanoparticles. Investigations presented, are performed mainly by AFM of the systems in thin film adsorbed on native oxide-terminated Si substrate. TEM was used to reveal the change in size of the obtained gold nanoparticles.

B. Mahltig (✉)
GMBU e.V.,
Postfach 520165,
01317 Dresden, Germany
e-mail: mahltig@gmx.de

J.-F. Gohy
Unité de Chimie des Matériaux Inorganiques et Organiques
(CMAT), Université catholique de Louvain (UCL),
Place Pasteur 1,
1348 Louvain-la-Neuve, Belgium

N. Cheval · A. Fahmi (✉)
School of Mechanical, Materials and Manufacturing Engineering,
The University of Nottingham,
University Park,
Nottingham NG7 2RD, UK
email: Amir.Fahmi@nottingham.ac.uk

Keywords Polyampholyte · Gold · Nanoparticles

Introduction

Polyelectrolytes are charged polymers recently have received not only high scientific interest but also have commercial impact in wide range of industrial applications such as paper production, wastewater treatment, washing powder and medical purposes [1–6]. In particular diblock of polyelectrolytes are of interest, since they containing one hydrophobic polymer block and one charged block. Therefore, they have the potential to use as additives for the preparation of metal nanoparticles. These copolymer additives are known for their templating effect, i.e. they restrict the growth of formed metal particles and control in this way the size and also the shape of the particles. Also the polymers act as stabilizer for the particles in respect to particle aggregation. By use of polyelectrolyte additives it is therefore possible to prepare stable metal particles of a predetermined size and size distribution [7–13]. Here, especially mentioned should be diblock polyelectrolytes of PEG-*b*-polyamine type (PEG for poly(ethylene)glycol). These double hydrophilic block copolymers are used as surface-modification agent to gain metal nanoparticles soluble in aqueous solvent. While the amino groups are coordinated to the metal surface, the hydrophilic PEG block is directed to the solvent. By this, a good solubility of metal particles in aqueous solvent is possible [14, 15].

Polyampholytes are a special type of polyelectrolytes carrying both negatively and positively charged functional groups on the same polymer chain. In case of weak polyampholytes the polymer contains acidic and alkaline groups and the polymer charge essentially depends on the pH of the solvent medium. Under appropriate conditions,

the functional groups dissociate, leaving ions on chains and counterions in solution. After ionization, positively and negatively charged groups are present on the polymer chain. The conformation of these polymers in solutions strongly depends on the distribution of charged monomers along the polymer backbone and their environment. In general the conformation of weak polyampholytes is very sensitive to acidic or alkaline additives [16–21].

While the chemistry and physics of polyampholytes are well understood, the use of polyampholytes as templates for the preparation of noble metal nanoparticles is little investigated. An example of this concept is found in the work reported by Note et al. [22] who investigated the effect of hydrophobically modified polyampholytes on the preparation of gold nanoparticles [22] and $BaSO_4$ particles [23]. The investigated polyampholyte contained a permanently positively charged block and a hydrophobically modified block with acidic groups. According to this previously reported paper, the question opens what effect on the formation of gold particles will have a simple weak diblock polyampholyte as function of polymer size and block ratio? To give an appropriate answer, we report here on the use of poly (methacrylic acid)-*block*-poly((dimethylamino)ethyl methacrylate), PMAA-*b*-PDMAEMA (Fig. 1), diblock polyampholytes as templates for the synthesis of gold nanoparticles. The adsorption behaviour of these polyampholytes at solid/liquid interfaces was previously intensively investigated [24–27].

The comparison of these polyampholytes with different block ratios and molecular weights will provide a good basis for understanding the influence of the polymer characteristic features during the formation of gold particles. The fabrication of gold nanoparticles will be realised in two different solvents which are DMF and THF. As gold source $HAuCl_4$ and as reductive agent $LiBH_4$ will be used.

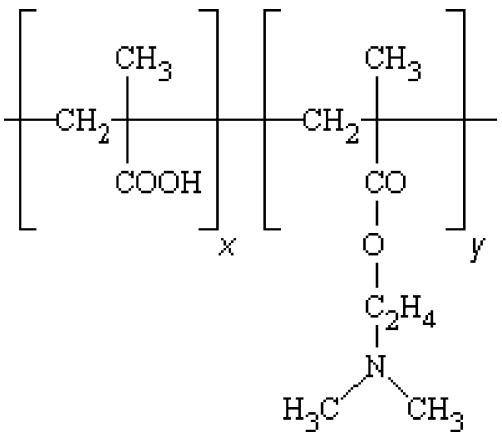

Fig. 1 Chemical structure of the PMAA-*b*-PDMAEMA polyampholyte, the block sizes *x* and *y* correspond to the degree of polymerisation given by M_n of polyampholyte and block ration (compare Table 1)

The influence of these precursors on the polyampholyte conformation will be investigated by AFM on thin film at air/solid interface while, the size of the accordingly obtained gold nanoparticles will be measured by TEM.

Experimental part

All investigations are performed with the diblock polyampholyte poly(methacrylic acid)-*block*-poly((dimethylamino)ethyl methacrylate), PMAA-*b*-PDMAEMA, with different molecular weight and block ratio (see Table 1). The synthesis of PMAA-*b*-PDMAEMA was performed by sequential anionic polymerization of *tert*-butylmethacrylate and dimethylamino)ethyl methacrylate followed by hydrolysis of the *tert*-butylmethacrylate units into methacrylic acid ones, as reported elsewhere [26, 28–30]. Following the polymer preparation and characterisation is described briefly. The monomers were purified by distillation over triethylaluminum. The glass reactor containing the required amount of LiCl (10/1 LiCl/initiator molar ratio) was flamed-dried under vacuum, purged with nitrogen, added with the solvent (tetrahydrofuran), and cooled to −78 °C. Diphenylmethyllithium was added dropwise until a persistent yellow color was observed, followed by the required amount of this initiator. *tert*-Butyl methacrylate was first polymerized at −78 °C for 1 h, followed by DMAEMA (2 h at −78 °C). A sample was picked out from the reactor before the addition of DMAEMA. The copolymerization reaction was then quenched with methanol. The characterization of the products was performed by size exclusion chromatography (SEC) and nuclear magnetic resonance (NMR). SEC was performed in tetrahydrofuran added with 1% (v/v) triethylamine, using a Hewlett-Packard 1050 liquid chromatograph equipped with two Plgel columns (1,000 and 10,000 Å, respectively) and a Hewlett-Packard 1047A refractive index detector. Poly(methyl methacrylate) standards were used for calibration. 1H NMR spectra were recorded at 400 MHz with Bruker AM 400 spectrometer. M_n of the second block was calculated from the 1H NMR spectrum of the copolymer and M_n of the first block. The tert-butyl methacrylate units were converted into methacrylic acid (MAA) by hydrolysis at the reflux of dioxane/HCl 9/1 v/v for 2 days. The final (co)polymers were purified by dialysis against regularly replaced distilled water for 2 weeks.

For preparation of gold nanoparticles, these polyampholytes were dissolved in DMF or THF. All the solutions were prepared at the same concentration of 1.4 mg/ml. Tetrachloroauric acid ($HAuCl_4$) which was used as precursor, was added to the polyampholyte solution to form the gold particles. This metal salt interacts with the DMAEMA monomer unit. An ionic interaction is created between the

Table 1 Characteristics of the investigated polyampholytes as determined by size exclusion chromatography (SEC) and nuclear magnetic resonance (NMR)—procedure detailed described in the experimental part

Polyampholyte	Molecular weight M_n (g/mol)	PMAA-*b*-PDMAEMA Weight ratio
A2	14,000	65/35
B2	62,000	55/45
B3	63,000	29/71
C1	101,000	44/56

metal salt and the DMAEMA monomer unit. The equimolar amount of gold precursor (m($HAuCl_4$)) was calculated between gold precursor and the DMAEMA monomer unit (1).

$$f.n(DMAEMA) = n(HAuCl_4)m(HAuCl_4) = f.\frac{M_n(PDMAEMA).m(PMAA/PDMAEMA).M_n(HAuCl_4)}{M_n(DMAEMA).M_n(PMAA/PDMAEMA)} \quad (1)$$

With f as the molar fraction between the $HAuCl_4$ and DMAEMA unit, M_n (PDMAEMA) the molecular weight of PDMAEMA block, m(PMAA-PDMAEMA) the mass of the block copolymer, M_n ($HAuCl_4$) the molecular weight of gold precursor (339.79 g/mol), M_n (DMAEMA) the molecular weight of DMAEMA monomer unit and M_n (PMAA-PDMAEMA) the molecular weight of PDMAEMA block. Gold particles were produced by the reduction of chloroaurate $[AuCl_4]^-$ using Lithiumborohydride ($LiBH_4$) dissolved in THF (2 M) as a reducing agent. Three drops of $LiBH_4$ solution were added to the solution to reduce the gold precursor. The colour changed from yellow to red dark indicating that the gold precursor is reduced to metallic gold nanoparticles. The experimental data for the preparation of the polyampholyte are presented in Table 2.

The microstructure of neat polyampholytes and Au/polyampholyte nanocomposites was characterised by AFM and TEM. Atomic force microscopy (AFM) (Dimension Nanoscope, VI, DI Santa Barbara) was used to investigate the topography in thin film after spin-coating on solid substrates. The measurements were performed in the tapping mode to minimize any damage to the sample surface. The size distribution of gold particles was studied by Transmission Electron Microscopy (TEM). Transmission electron microscopy (TEM) measurements were performed with a TECNAI Biotwin (FEI Ltd.) transmission electron microscope at 100 keV using carbon-coated copper grids (400 mesh, AGAR Scientific) to determine the size distribution of particles. The instrument was operated at low beam intensities to prevent electron damage of the polymer samples.

Results and discussion

Conformation of polyampholytes in different organic solvents

The PMAA-*b*-PDMAEMA polyampholytes were dissolved in DMF or THF and spin coated on a silicon substrate to obtain a thin film. Atomic force microscopy was used to observe the surface of the substrate. For the B2 and C1 polyampholytes dissolved in DMF, the surface of the substrate is covered with a block copolymer layer and some larger aggregates are observed (Figs. 2b and d). The aggregation of the block copolymer can be explained on the basis of specific interactions developing between the PMAA and PDMAEMA blocks. Indeed, in a recent report, the formation of hydrogen bonds between weak polyacid and polybase blocks was investigated in DMF and THF [31]. In this report, the polyacid was polyacrylic acid (PAA) and the polybase poly(4-vinylpyridine) (P4VP). Partial proton transfer and/or hydrogen-bonding was evidenced between PAA and P4VP, leading to the formation of PAA/P4VP complexes. The solubility of those complexes depended on the length of the interacting blocks and was modulated by the used solvent. In this respect, longer interacting blocks led to less soluble complexes and the complexes were more soluble in DMF than in THF. Similar non-covalent interactions could occur in the PMAA-*b*-PDMAEMA investigated in the present study. Moreover, proton transfer and/or hydrogen bonding could occur between the carboxylic acid group of PMAA and the amino-group of PDMAEMA leading to either intra- or interchain aggregation. Those interactions would be maximized for PMAA-*b*-PDMAEMA samples in which the number of MAA and DMAEMA units are about the same (symmetric polyampholytes), leading to large aggregated structures in solution. This is actually the case

Table 2 Solutions of polyampholytes dissolved in DMF and THF

Polyampholyte	Volume of solvent (ml)	Weight of polyampholyte (mg)	Weight $HAuCl_4$ (mg)
A2	10	14	5.30
B2	10	14	6.82
B3	10	14	10.57
C1	10	14	8.5

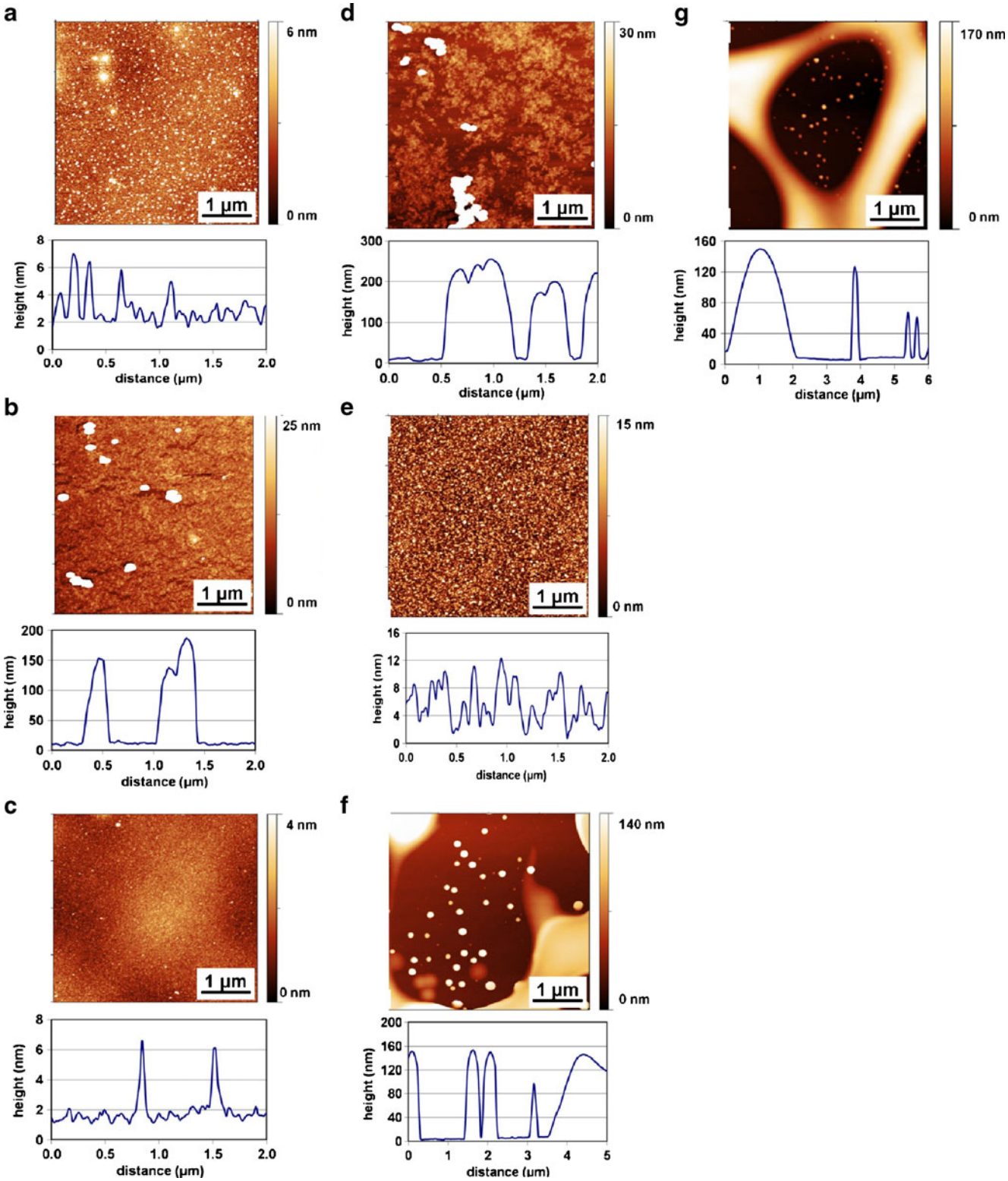

Fig. 2 AFM images of polyampholyte solutions after spin-coating onto silicon substrates; **a** to **d** polyampholytes dissolved in DMF; **e** to **g** polyampholytes dissolved in THF

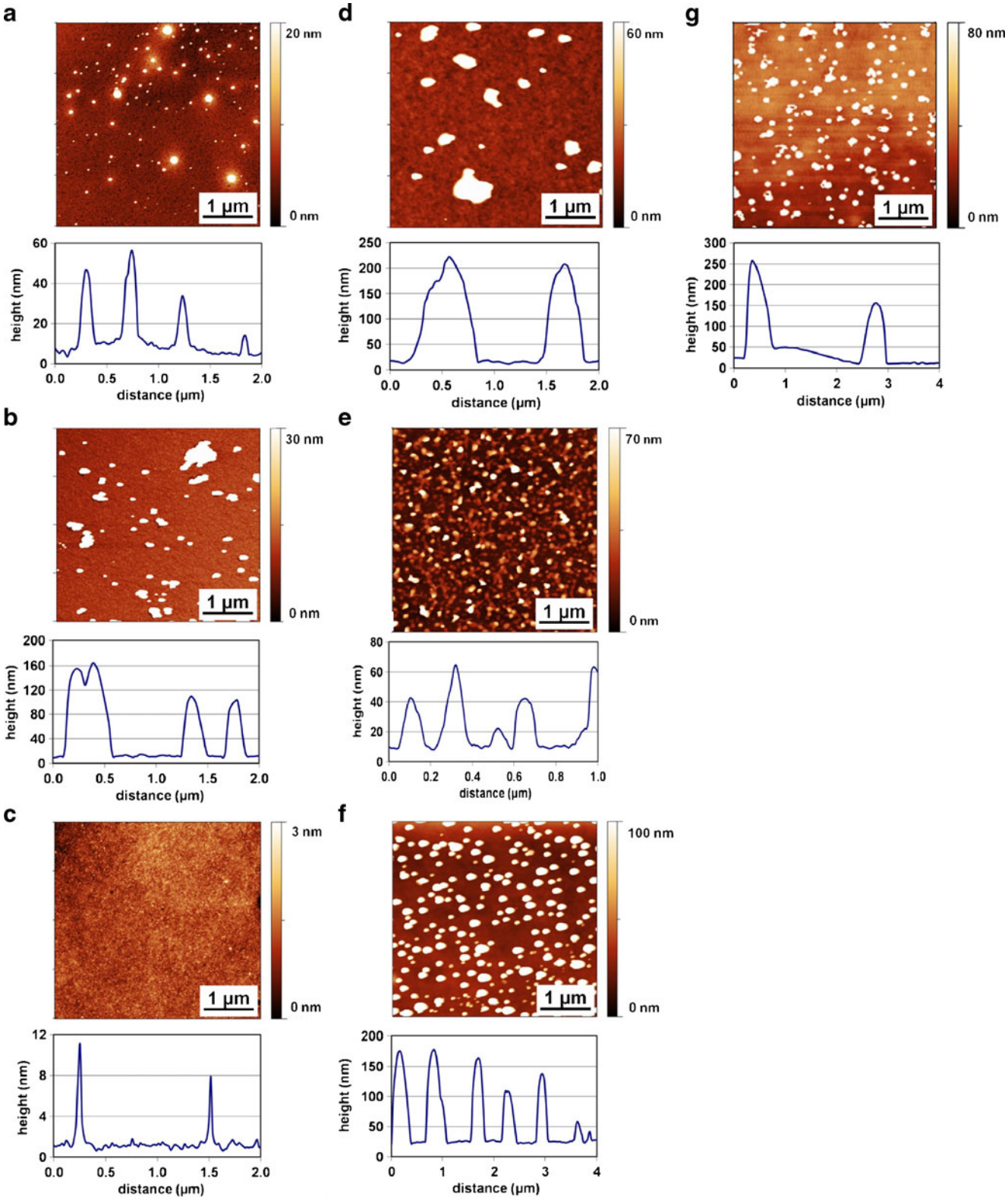

Fig. 3 AFM images of polyampholyte solutions with gold precursor $HAuCl_4$ after spin-coating onto silicon substrates; **a** to **d** polyampholytes dissolved in DMF; **e** to **g** polyampholytes dissolved in THF

Table 3 The arithmetic mean roughness for polyampholyte solutions spin-coated on silicon substrates as determined by AFM

No.	Polyampholyte *PMAA-b-PDMAEMA* in DMF			Polyampholyte *PMAA-b-PDMAEMA* in THF		
	Ra Neat polyampholyte	Ra Polyampholyte with $HAuCl_4$	Ra Polyampholyte with Au	Ra Neat polyampholyte	Ra Polyampholyte with $HAuCl_4$	Ra Polyampholyte with Au
A2	5.5	25	7	6	30	30
B2	75	85	101	74	76	85
B3	3	4.5	14	unsoluble	unsoluble	unsoluble
C1	103	100	108	70	74	90

for the B2 and C1 samples that are characterized by a nearly symmetric composition (see Table 1) and are thus characterized by globular polyampholyte conformation in solution. This is in agreement with the aggregates of B2 and C1 block copolymers that can be observed on the silicon substrate (Figs. 2b and d). The roughness of the block copolymer thin film on the silicon substrate is significantly high for these two samples. The arithmetical mean roughness *(Ra)* is about 80 nm for B2 and 110 nm for C1.

For the A2 and B3 polyampholytes, a smooth film and some micelles cover the silicon substrate (Figs 2a and c). For A2, Ra is about 2.5 nm while for B3; the arithmetical mean roughness is around 3 nm. The morphology of the polyampholyte on the substrate can be explained by the asymmetric composition of the A2 and B3 samples. For A2 containing a bigger PMAA block, the growth of the aggregated structures resulting from the aggregation of the insoluble PMAA/PDMAEMA non covalent complexes could be modulated by the excess of uncomplexed PMAA chain segments. For B3 containing a bigger PDMAEMA block, the PMAA/PDMAEMA insoluble complexes could be stabilized by the excess of uncomplexed PDMAEMA chain segments. In both cases, the formation of micellar aggregates in DMF could be anticipated. Those micelles would be formed of an insoluble PMAA/PDMAEMA complex core surrounded by either PMAA (in case of A2) or PDMAEMA (in case of B3) coronal chains. Those micelles would then form the smooth films observed in Fig. 2 after spin coating. This hypothesis is credited by the observation of small micelles on top of a dense micellar film as observed in Fig. 2.

In previous study on PAA/P4VP complexes, it was concluded that the solubility of those complexes was reduced when THF was used instead of DMF [31]. This behaviour was related to the different abilities of THF and DMF to form competing hydrogen bonds with the PAA/P4VP complexes. The same situation could be anticipated for the PMAA-*b*-PDMAEMA polyampholytes studied here.

As the A2, B2 and C1 polyampholytes can be dissolved in THF, but not the B3 sample. This could be accounted by the composition of the B3 sample that contains a majority of DMAEMA units. Since both DMAEMA units and THF contains acceptors moieties (lone pairs) for hydrogen bonds, one can easily understand that the solubility of the B3 sample will be restricted in THF due to the lack of H-donating groups (which are indeed the MAA groups). In sharp contrast, the solubility of the A2 polyampholyte should be considerably better than the B3 sample since A2 contains an excess of PMAA chain segments prone to form hydrogen bonds with THF. This is clearly demonstrated in Fig. 2e in which a dense film of micelles are visualized onto the silicon substrate.

In case of the "symmetric" B2 and C1 samples, one could expect a reduced solubility of the PMAA/PDMAEMA complexes in THF compared to DMF, in agreement with the previously reported results [31]. Indeed, very large aggregated structures are observed after spin-coating the solutions onto a silicon substrate (see Fig. 2f and g) in agreement with a reduced solubility of the PMAA/PDMAEMA complexes in THF.

In this section, we have thus demonstrated that the conformation of the PMAA-*b*-PDMAEMA polyampholytes is controlled by the formation of PMAA/PDMAEMA non-covalent complexes. The solubility of these complexes can be controlled by the used organic solvents and also by the presence of an excess of uncomplexed PMAA or PDMAEMA chain segments.

Influence of gold precursor on polyampholyte conformation

From a practical point of view, the amount of gold precursor was calculated for a ratio of 1:1 with respect to the DMAEMA monomer unit (Table 2). The fabrication of gold nanoparticles was realised in DMF and in THF. Firstly, $HAuCl_4$ was added to the polyampholyte solutions in DMF or THF. Secondly, the reduction of the gold precursor by $LiBH_4$ was performed.

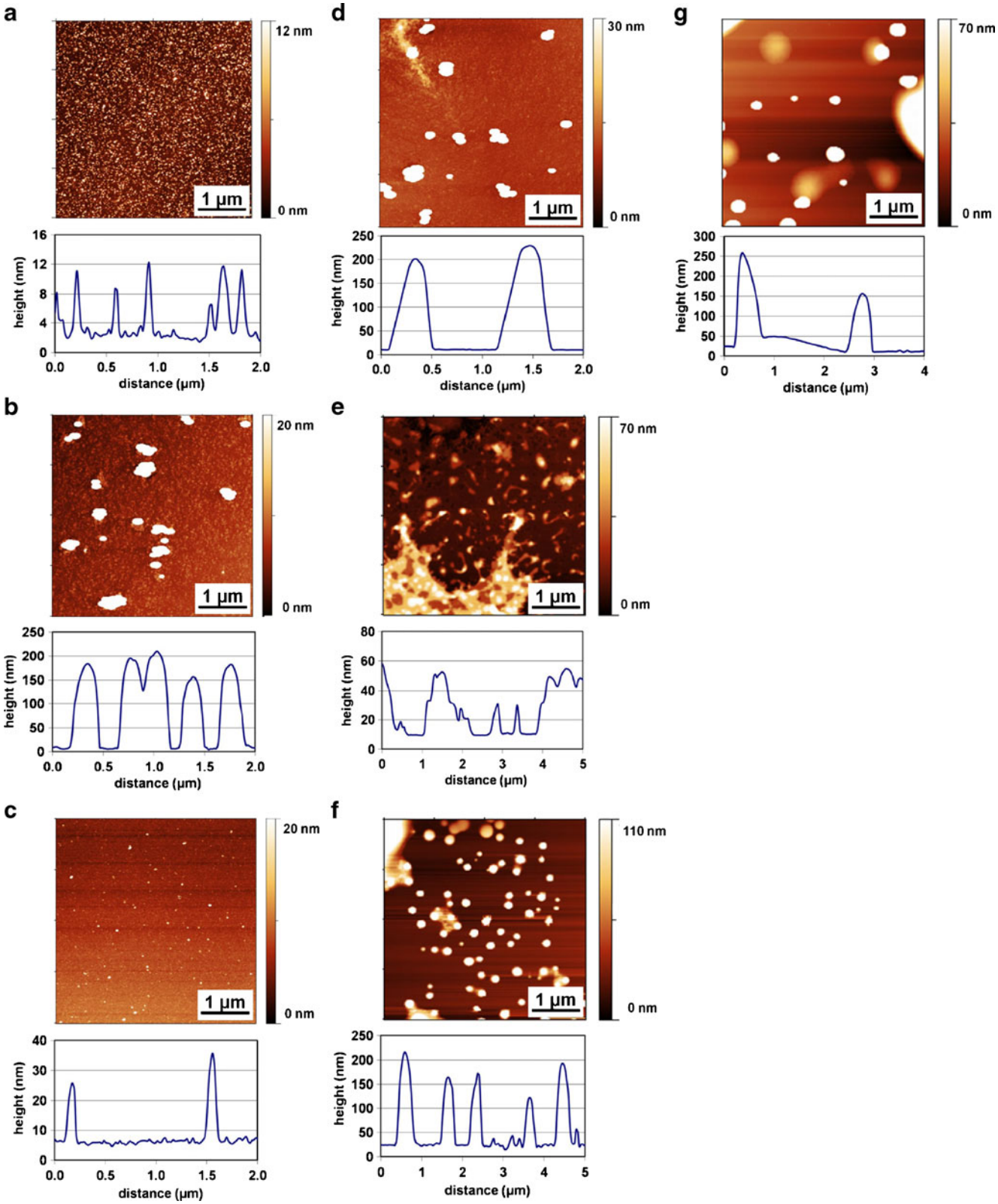

Fig. 4 AFM images of polyampholyte solutions with gold particles after spin-coating onto silicon substrates; **a** to **d** polyampholytes dissolved in DMF; **e** to **g** polyampholytes dissolved in THF

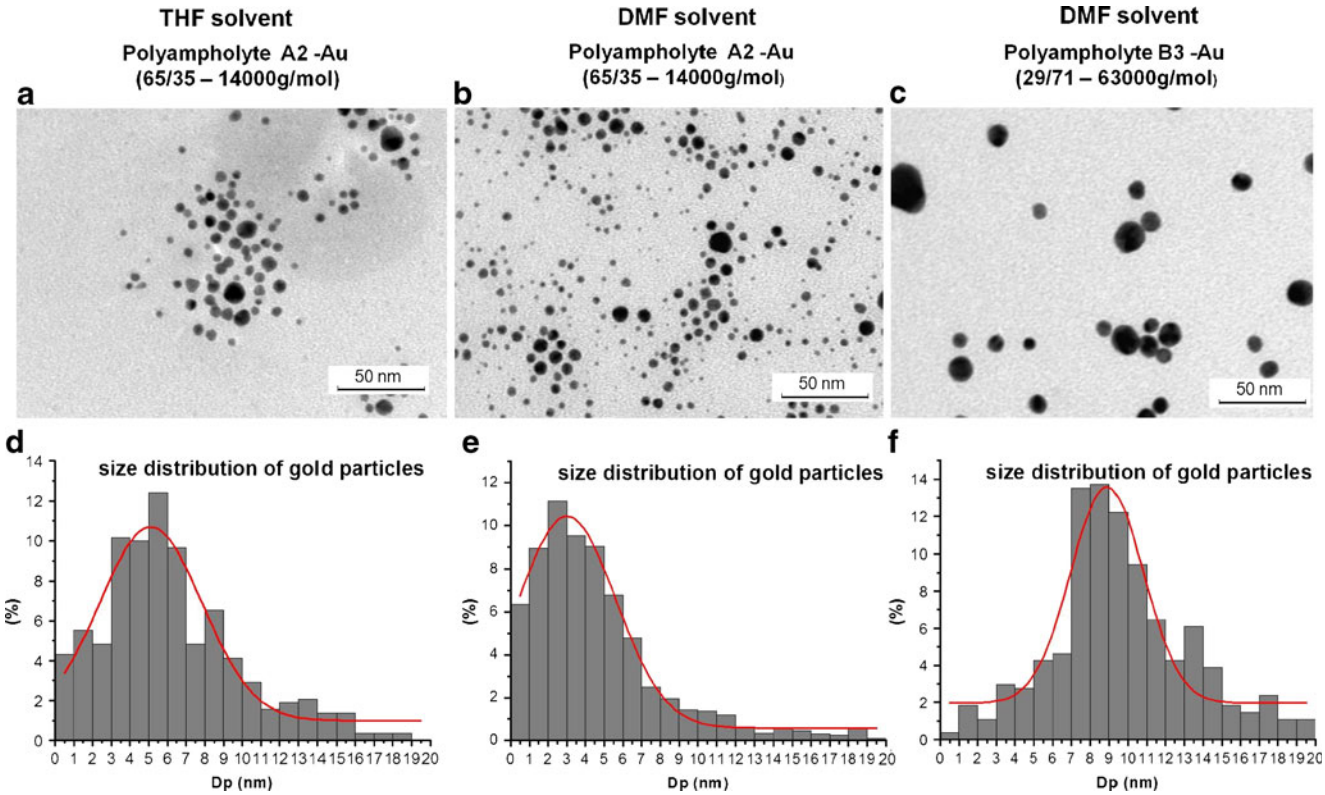

Fig. 5 TEM images and related particle size distribution of gold nanoparticles prepared in different polyampholyte solutions

The introduction of precursors of gold nanoparticles into polyampholyte solutions is expected to modify the conformation of the latter. Indeed, the added gold salt ($HAuCl_4$) is able to interact with the DMAEMA units of the polyampholyte. In this respect an acid-base reaction will occur between these two partners resulting in protonation of the amino group of DMAEMA. This protonation will further eliminate the possibility of DMAEMA units to form complexes with MAA units and will introduce positive charges (and thus electrostatic repulsions) among PDMAEMA blocks.

For A2 dissolved in DMF, the conformation of the block copolymer has changed due to this protonation. The aggregation of block copolymer has been observed on the surface of the substrate after adding the gold precursor instead of a smooth surface (Fig. 3a). The arithmetical mean roughness of the polyampholyte A2 at substrate surface has increased also after adding the gold precursor. The arithmetical mean roughness *(Ra)* is about 5.5 nm for the neat polyampholyte and around 25 nm after adding the gold precursor (Table 3). The small micelles that were observed on top of the polymer films (Fig. 2a) have also disappeared after protonation of the DMAEMA units. For the polyampholyte B2, B3 and C1 dissolved in DMF, the protonation of the PDMAEMA blocks has almost no influence on the chain conformation. The arithmetical mean roughness *(Ra)* for these three polyampholytes is approximately the same after adding the gold precursor (Table 3). From these observations, it is not clear to see whether the initial insoluble PMAA/PDMAEMA noncovalent complexes have been disrupted or not by protonation of the PDMAEMA block.

The influence of acidification in the solution is more important for the polyampholytes dissolved in THF. This could be accounted by the reduced solubility of charged protonated PDMAEMA blocks in THF compared to DMF. Since the dielectric constant of THF is much lower than the one of DMF, one could assume that electrostatic interactions are maximized in THF leading to aggregated structures in which the charged PDMAEMA blocks form the core. Such a structure will be similar to the so-called reversed micelles in which ion pairs are included into the micellar core. Once again, no stable structure is observed for the B3 sample since it contains a majority of aggregating protonated PDMAEMA blocks and a minority of PMAA stabilizing blocks. For the three other investigated copolymers, dense aggregates with a size around 100 nm have been observed. Those structures could correspond to aggregated protonated PDMAEMA cores surrounded by PMAA stabilizing chains. The smallest structures have been observed for the A2 sample in agreement with the short PDMAEMA block found in this sample (see Table 2).

Formation of gold nanoparticles in presence of polyampholyte

After adding the reducing agent to the polyampholyte solution containing gold precursor, all solutions were spin coated and observed by AFM (see Fig. 4). Except for sample A2, the results obtained before and after formation of the gold nanoparticles are quite similar independent which of both solvent is used (compare Figs. 3 and 4a, d data in Table 3). This means that the conformation of the PMAA-*b*-PDMAEMA block polyampholyte is not much affected by the formation of the gold nanoparticles. This also explains that the formed nanoparticles are much smaller than the size of the aggregated structures found in the polyampholytes. According to the micellar aggregate model proposed before with a protonated PDMAEMA core and a PMAA core, one could assume that the gold nanoparticles are essentially located into the PDMAEMA core that for this plays the role of templating locus. This statement is in agreement with results gained with PEG-*b*-polyamines and gold nanoparticles reported earlier in literature [14, 15]. In case of PEG-*b*-polyamine diblock copolymer it is supposed that the amino containing block is directed to the gold particles and a multipoint coordination of tertiary amino groups on the gold surface leads to stable modification.

For the A2 sample, it is interesting to note than the ill-defined structures found after acidification of the solution (Fig. 3a) collapses to compact micellar structures after gold nanoparticle formation (Fig. 4a). Those structures are similar to the ones initially observed in the unloaded A2 sample (Fig. 2a). This can be understood on the basis of the short PDMAEMA blocks found in this copolymer. These blocks are too short to from well defined micellar structures with protonated PDMAEMA cores. However, these chains could densify once they are hold together by gold nanoparticles. This observation also suggests that smaller gold nanoparticles would be obtained while using the lower molecular weight A2 samples compared to the three other investigated polyampholytes.

The size distribution of gold was investigated with TEM. Polyampholyte B3 with gold in THF and polyampholyte A2 with gold in THF and DMF were observed. The type of solvent has an impact on the particle size of the gold nanoparticle. Indeed, for the polyampholyte A2, the size of gold particles is bigger in THF solvent than in DMF solvent. The average size of gold is around 5.1 nm±2.7 in THF and 3 nm±2.6 in DMF (Fig. 5). The size of gold particles is bigger in THF because the aggregation of the PDMAEMA blocks is greatly enhanced in low polarity THF compared to DMF, as previously discussed. Moreover, the volume fraction between PMAA and PDMAEMA blocks and the molecular weight have an influence on the size of gold particles. In fact, the A2 and B3 polyampholytes have a different volume fraction and molecular weight (Table 1), so in presence of these two polyampholytes, the size of formed gold particles is different. For A2, the average size is around 3 nm±2.6 while for B3, the size is about 8.9 nm±4.5 (Fig. 5). The size of gold particles in the polyampholyte C1 is bigger than the polyampholyte B3 because in C1, the volume fraction of PMAEMA is high and the polyampholyte chain is long. The equi-molar amount of gold precursor (m($HAuCl_4$)) was calculated between gold precursor and the DMAEMA monomer unit. Then, the number of gold particles is more important on the polyampholyte C1 due to the high volume fraction of PDMAEMA block and to the high molecular weight of block copolymer which facilitate the aggregation of gold particles. Therefore, the size of the gold particles increases as function of the size of PDAEMA blocks and the molecular weight of the polyampholyte.

Conclusions

The comparison of the polyampholytic system—poly(methacrylic acid)-*block*-poly((dimethylamino)ethyl methacrylate), PMAA-*b*-PDMAEMA—with different block ratios and molecular weights provides a good basis for understanding the influence of polyampholyte during the formation of gold particles. The fabrication of gold nanoparticles was realised in two different solvents which are DMF and THF. As gold precursor $HAuCl_4$ and as reductive agent $LiBH_4$ were used. The influence of the metal precursor and the reduction agent on the polyampholyte conformation was investigated by AFM. It was found that the conformation of the weak polyampholyte was strongly affected during preparation of the gold nanoparticles, probably by the protonation of the PDMAEMA blocks during the preparation process. Moreover, the size of the gold nanoparticles is significantly influenced by changing the polarity of the used solvent, the volume ratio between PDMAEMA and PMAA blocks and by the molecular weight.

Acknowledgments JFG is grateful to the ESF STIPOMAT Programme and to BELSPO for financial support in the frame of the network IAP 6/27. We also acknowledge the financial support of the UK EPSRC through the Nottingham NIMRC.

References

1. Böhm N, Kulicke W-M (1997) Colloid Polym Sci 275:73–81
2. Duivenvoorde FL, van Nostrum CF, van der Linde R (1999) Prog Org Coat 36:225–230
3. Claesson PL, Dahlgren MAG, Erikson L (1994) Colloids Surf A 93:293–295
4. Buchhammer H-M, Petzold G, Lunkwitz K (1999) Langmuir 15:4306–4310

5. Henderson KF (ECC Int Inc) (1998) World Patent 0034581(A1)
6. Musabekov KB, Tusupbaev NK, Kudaibergenov SE (1998) Macromol Chem Phys 199:401–408
7. Svergun DI, Shtykova EV, Dembo AT, Bronstein LM, Platonova OA, Yakunin AN, Valetsky PM, Khokhlov AR (1998) J Chem Phys 109:11109–11116
8. Bronstein LM, Platonova OA, Yakunin AN, Yanovskaya IM, Valetsky PM, Dembo AT, Obolonkova ES, Makhaeva EE, Mironov AV, Khokhlov AR (1999) Colloids Surf A 147:221–231
9. Zhao F, Xu J (2006) Colloid Polym Sci 285:113–117
10. Tang X-L, Jiang P, Ge G-L, Tsuji M, Xie S-S, Guo Y-J (2008) Langmuir 24:1763–1768
11. Jewrajka SK, Chatterjee U (2006) J Polymer Sci A: Polym Chem 44:1841–1854
12. Sun X, Dong S, Wang E (2005) Langmuir 21:4710–4712
13. Mahltig B, Gutmann E, Reibold M, Meyer DC, Böttcher H (2009) J Sol-Gel Sci Technol 51:204–214
14. Ishii T, Otsuka H, Kataoka K, Nagasaki Y (2004) Langmuir 20:561–564
15. Miyamoto D, Oishi M, Kojima K, Yoshimoto K, Nagasaki Y (2008) Langmuir 24:5010–5017
16. Dobrynin AV, Ralph H, Colby RH, Rubinstein M (2004) J Polym Sci 42:3513–3538
17. Kudaibergenov SE (1999) Adv Polym Sci 144:115–197
18. Moldakarimov SB, Kramarenko EY, Khokhlov AR, Kudaibergenov SE (2001) Macromol Theory Simul 10:780–788
19. Wang Z, Rubinstein M (2006) Macromolecules 39:5897–5912
20. Kudaibergenov SE, Ciferri A (2007) Macromol Rapid Commun 28:1969–1986
21. Ulrich S, Seijo M, Stoll S (2007) J Phys Chem B 111:8459–8467
22. Note C, Koetz J, Wattebled L, Laschewsky A (2007) J Colloid Interf Sci 308:162–169
23. Note C, Ruffin J, Tiersch B, Koetz J (2007) J Dispersion Sci Technol 28:155–164
24. Mahltig B, Gohy J-F, Jérôme R, Stamm M (2001) J Polym Sci Part B: Polym Phys 39:709–718
25. Mahltig B, Gohy J-F, Jérôme R, Pfütze G, Stamm M (2003) J Polym Res 10:69–77
26. Mahltig B, Jérôme R, Stamm M (2003) J Polym Res 10:219–223
27. Mahltig B, Werner C, Müller M, Jérôme R, Stamm M (2001) J Biomater Sci Polymer Edition 12:995–1010
28. Creutz S, Teyssié P, Jérôme R (1997) Macromolecules 30:6–9
29. Creutz S, van Stam J, Antoun S, De Schryer FC, Jérôme R (1997) Macromolecules 30:4078–4083
30. Antoun S, Teyssié P, Jérôme R (1997) Macromolecules 30:1556–1561
31. Lefèvre N, Fustin C-A, Varshney SK, Gohy J-F (2007) Polymer 48:2306–2311